

# Fermi Surface, Surface States, and Surface Reconstruction in $\text{Sr}_2\text{RuO}_4$

A. Damascelli, D.H. Lu, K.M. Shen, N.P. Armitage, F. Ronning, D.L. Feng, C. Kim, and Z.-X. Shen

*Department of Physics, Applied Physics and Stanford Synchrotron Radiation Lab., Stanford University, Stanford, CA 94305*

T. Kimura, and Y. Tokura

*Department of Applied Physics, The University of Tokyo, Tokyo 113-8656, and JRCAT, Tsukuba, 305-0046, Japan*

Z.Q. Mao, and Y. Maeno

*Department of Physics, Kyoto University, Kyoto 606-8502, and CREST-JST, Kawagushi, Saitama 332-0012, Japan*

(2 May 2000)

The electronic structure of  $\text{Sr}_2\text{RuO}_4$  is investigated by high angular resolution ARPES at several incident photon energies. We address the controversial issues of the Fermi surface (FS) topology and of the van Hove singularity at the M point, showing that a surface state and the replica of the primary FS due to  $\sqrt{2} \times \sqrt{2}$  surface reconstruction are responsible for previous conflicting interpretations. The FS thus determined by ARPES is consistent with the de Haas-van Alphen results, and it provides information on the detailed shape of the  $\alpha$ ,  $\beta$  and  $\gamma$  sheets.

PACS numbers: 74.25.Jb, 74.70.Ad, 79.60.Bm

Angle resolved photoemission spectroscopy (ARPES) has proven itself to be an extremely powerful tool in studying the electronic structure of correlated electron systems. In particular, in the case of high-temperature superconductors, it has been very successful in measuring the superconducting gap, determining the symmetry of the order parameter and characterizing the pseudo-gap regime [1]. On the other hand one of the fundamental issues, namely the determination of the Fermi surface (FS) topology, has been controversial, as in the case of  $\text{Bi}_2\text{Sr}_2\text{CaCu}_2\text{O}_8$ , raising doubts concerning the reliability of the ARPES results. A similar controversy has also plagued the fermiology of  $\text{Sr}_2\text{RuO}_4$ . In this context, the latter system is a particularly interesting case because it can also be investigated with de Haas-van Alphen (dHvA) experiments, contrary to the cuprates, thus providing a direct test for the ARPES results.

Whereas dHvA analysis, in agreement with LDA band-structure calculations [2,3], indicates two electronlike FS ( $\beta$ , and  $\gamma$ ) centered at the  $\Gamma$  point, and a hole pocket ( $\alpha$ ) at the X point [4–6], early ARPES measurements suggested a different picture: one electronlike FS ( $\beta$ ) at the  $\Gamma$  point and two hole pockets ( $\gamma$ , and  $\alpha$ ) at the X point [7,8]. The difference comes from the detection by ARPES of an intense, weakly dispersive feature at the M point just below  $E_F$ , that was interpreted as an extended van Hove singularity (evHS) pushed down below  $E_F$  by electron-electron correlations [7,8]. With the evHS below  $E_F$ , rather than above (LDA band-structure calculations place it 60 meV above  $E_F$  [2,3]), the  $\gamma$  pocket is converted from electronlike to holelike. The existence of the evHS was questioned in a later photoemission paper [9], where it was suggested that dHvA and ARPES results could be reconciled by assuming that the feature detected by ARPES at the M point was due to a sur-

face state (SS). Very recently, two possible explanations have been proposed: first, the evHS at the M point could be only slightly above  $E_F$  (e.g., 10 meV), so that considerable spectral weight would be detected just below  $E_F$  [10]. Alternatively, ARPES could also be probing ferromagnetic (FM) correlations reflected in two different  $\gamma$ -FS (hole and electronlike, respectively, for majority and minority spin direction), which escaped detection in dHvA experiments [11]. The resolution of this controversy is important not only for the physics of  $\text{Sr}_2\text{RuO}_4$  *per se*, but also as a reliability test for FS's determined by ARPES, especially on those correlated systems where photoemission is the only available probe.

In this paper, we present a detailed investigation of the electronic structure of  $\text{Sr}_2\text{RuO}_4$ . By varying the incident photon energy and the temperature at which the samples were cleaved, we confirm the SS nature of the near- $E_F$  peak detected at the M point, and we identify an additional dispersive feature related to the ‘missing’ electronlike FS ( $\gamma$ ). A complete understanding of the data can be achieved only by recognizing the presence of shadow bands (SB), due to a  $\sqrt{2} \times \sqrt{2}$  surface reconstruction which takes place on cleaved  $\text{Sr}_2\text{RuO}_4$  (as confirmed by LEED). The FS as determined by ARPES is consistent with the dHvA results [4–6], and it provides information on the shape of the  $\alpha$ ,  $\beta$  and  $\gamma$  sheets.

ARPES data was taken at SSRL on the normal incidence monochromator beam line equipped with a SES-200 electron analyzer in angle resolved mode. With this configuration it is possible to simultaneously measure multiple energy distribution curves (EDC's) in an angular window of  $\sim 12^\circ$ , obtaining energy-momentum information not at one single  $k$ -point but along an extended cut in  $k$ -space. The angular resolution was  $0.5^\circ \times 0.3^\circ$  [ $0.3^\circ$  along the cut, corresponding to a  $k$  resolution of 1.5% of

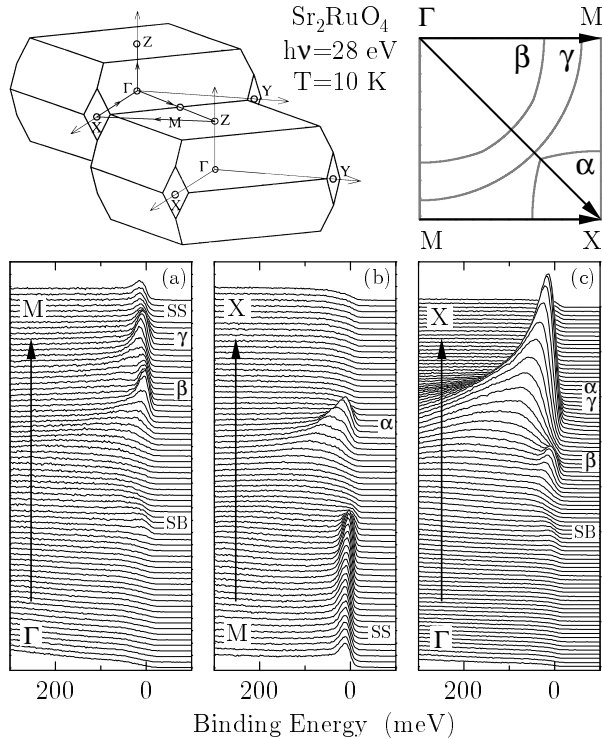


FIG. 1. ARPES spectra from  $\text{Sr}_2\text{RuO}_4$  along the high-symmetry lines  $\Gamma$ -M, M-X, and  $\Gamma$ -X. As shown in the sketch of the 3D BZ, M is the midpoint along  $\Gamma$ -Z and, together with  $\Gamma$  and X, defines the 2D projected zone (PZ). In the quadrant of the 2D PZ the  $\alpha$ ,  $\beta$  and  $\gamma$  sheets of FS are indicated together with the experimentally measured cuts.

the Brillouin zone (BZ), with 28 eV photons]. The energy resolution was 14 meV for high-symmetry cuts and photon energy dependence, and 21 meV for the FS mappings.  $\text{Sr}_2\text{RuO}_4$  single crystals were oriented by Laue diffraction, and then cleaved *in situ* with a base pressure better than  $5 \times 10^{-11}$  torr. In order to compensate for the angular response of the analyzer, EDC's in a single cut were normalized against those measured on polycrystalline gold. Different cuts were then normalized with respect to each other on the basis of the spectral weight above  $E_F$  integrated in both momentum and energy.

In order to begin the discussion of our experimental results, let us first give an overview of the very rich photoemission spectra, introducing all the features we will focus on throughout the paper. Fig. 1 presents EDC's along the high-symmetry directions for  $\text{Sr}_2\text{RuO}_4$  cleaved and measured at 10 K. The  $\alpha$ ,  $\beta$ , and  $\gamma$  sheets of FS expected on the basis of LDA calculations [2,3], and dHvA experiments [4–6] are indicated together with the experimentally measured cuts in the sketch depicting 1/4 of the 2D projected zone (PZ). All the features in the data are labeled following the assignments which will be given in the paper. Along  $\Gamma$ -M, two peaks emerge from the background, disperse towards  $E_F$ , and cross it before the M point, defining  $\beta$  and  $\gamma$  electronlike pockets (Fig. 1a).

Along M-X, a peak approaches and crosses  $E_F$  before the X point defining, in this case, the  $\alpha$  hole pocket centered at X (Fig. 1b). Similar results were obtained along  $\Gamma$ -X (Fig. 1c): the  $\beta$  pocket is clearly resolved, while  $\alpha$  and  $\gamma$  crossings are almost coincident. In addition, we identify a weak feature which shows a dispersion opposite to the primary peaks along  $\Gamma$ -M and  $\Gamma$ -X (SB, see below). Around the M point a sharp peak is observed (SS), whose weak dispersion along M-X can be followed until it crosses  $E_F$  and loses intensity. The highest binding energy along the dispersion (which is symmetric with respect to  $\Gamma$ -M) is found at the M point. Because of this behavior, the SS peak was initially associated to a sheet of FS centered at X, and holelike in character [7].

In the following discussion, we will concentrate on the features observed near the M point, which are relevant to the controversy concerning the character of the  $\gamma$  sheet of FS. We will show that with sufficient momentum resolution, and in particular with 28 eV photons, both the  $\beta$  and  $\gamma$  electronlike pockets (predicted by LDA calculations [2,3]) are clearly resolved in the ARPES spectra. We measured the M point region (with cuts along  $\Gamma$ -M- $\Gamma$ ) varying the incident photon energy between 16 and 29 eV, in steps of 1 eV. Here, we covered the location of  $\beta$  and  $\gamma$  pockets in both first and second zone for better illustration (i.e., four  $E_F$  crossings will be observed). From the EDC's shown in Fig. 2 for 16, 22, and 28 eV, we can see that the cross sections of SS,  $\beta$  and *in particular*  $\gamma$  exhibit a strong (and different) dependence on photon energy (note that by working at lower photon energies the momentum resolution increases and, in turns, the number of EDC's becomes progressively larger in going from panel c to a). At 28 eV,  $\beta$  and  $\gamma$  crossings can be individually identified in the EDC's. Owing to the high momentum resolution we can now follow the dispersion of the  $\gamma$  peaks until the leading edge midpoints are lo-

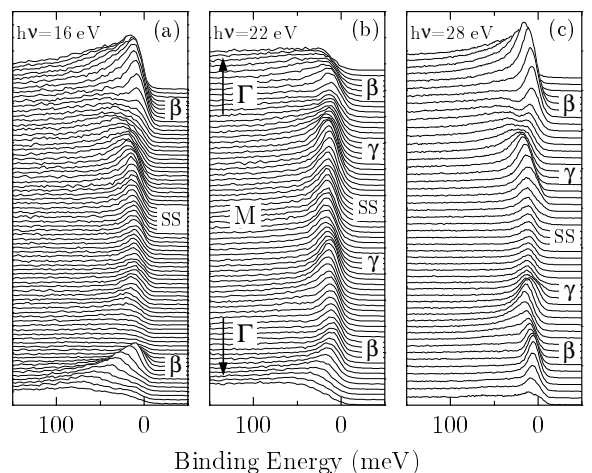


FIG. 2. ARPES spectra along  $\Gamma$ -M- $\Gamma$ , at three different photon energies. The cuts are centered at the M point and extend beyond the  $\gamma$  and  $\beta$  FS in both first and second zone.

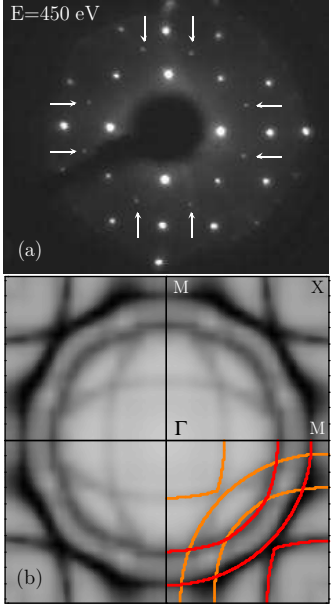


FIG. 3. Panel a: LEED pattern measured at 10 K with 450 eV electrons. The arrows indicate superlattice reflections due to  $\sqrt{2} \times \sqrt{2}$  surface reconstruction. Panel b: Fermi energy intensity map. Primary  $\alpha$ ,  $\beta$  and  $\gamma$  sheets of FS are marked by red lines, and replica due to surface reconstruction by yellow lines. All data was taken on  $\text{Sr}_2\text{RuO}_4$  cleaved at 10 K.

cated beyond  $E_F$ . After that, the peaks lose weight and disappear, defining the  $k_F$  vectors for the electronlike  $\gamma$  pockets. Right at  $k_F$  we can resolve a double structure which then reduces to the non dispersive feature (SS) located 11 meV below  $E_F$ . The difference between the 28 eV results and those obtained at 16 or 22 eV is striking (the latter are consistent with those previously reported at similar photon energies [7,8]). At low photon energies, the  $\beta$  crossings are still clearly visible. On the other hand, we can follow only the initial dispersion of the  $\gamma$  peaks (now broad and weak), before they merge with the SS feature, giving the impression of an evHS. At 16 eV it is impossible to identify the  $\gamma$  crossings. At 22 eV the location of the leading edge midpoints is at best suggestive of the presence of the  $\gamma$  crossings.

We showed that the  $\gamma$  electron pocket had so far escaped detection in ARPES because it is indistinguishable from the SS feature at low photon energy and/or low angular resolution. In order to have a full picture of the relevant issues to be addressed, let us proceed to the discussion of the FS mapping. Fig. 3b shows the  $E_F$  intensity map obtained at 28 eV on a  $\text{Sr}_2\text{RuO}_4$  single crystal cleaved and measured at 10 K. The actual EDC's were taken over more than a full quadrant of the PZ with a resolution of  $0.3^\circ$  ( $1^\circ$ ) in the horizontal (vertical) direction. The EDC's were then integrated over an energy window of  $\pm 10$  meV about the chemical potential. The resulting map of  $73 \times 22$  points was then symmetrized with respect to the diagonal  $\Gamma$ -X (to compensate for the different res-

olutions along horizontal and vertical directions). The  $\alpha$ ,  $\beta$ , and  $\gamma$  sheets of FS are clearly resolved, and are marked by red lines in Fig. 3b. In addition, Fig. 3b shows some unexpected features: besides the diffuse intensity around the M point due to the presence of the SS band, there are weak but yet well defined profiles (marked in yellow). They can be recognized as a replica of the primary FS, and are related to the weak SB features detected in the EDC's along the high-symmetry lines (Fig. 1a and 1c). This result is reminiscent of the situation found in  $\text{Bi}_2\text{Sr}_2\text{CaCu}_2\text{O}_8$  where similar shadow bands are possibly related to AF correlations, or to the presence of two formula units in the unit cell [1]. On the other hand, in  $\text{Sr}_2\text{RuO}_4$  the origin of the SB is completely different: inspection with LEED reveals superlattice reflections corresponding to a  $\sqrt{2} \times \sqrt{2}$  surface reconstruction (see Fig. 3a), which is responsible for the folding of the primary electronic structure with respect to the M-M direction. This reconstruction, which was found on all the  $\text{Sr}_2\text{RuO}_4$  samples, is absent in the cuprates. Quantitative LEED analysis of the surface structure shows a  $9^\circ$  rotation of the  $\text{RuO}_6$  octahedra around the surface normal, which leads to the enlargement of the in-plane unit-cell dimensions by  $\sqrt{2} \times \sqrt{2}$  over that of the bulk [12]. This reconstruction, which reveals an intrinsic instability of the cleaved surface, should be taken into account as the origin of possible artifacts in all surface sensitive measurements.

By inspecting the M point (Fig. 3b), it becomes now clear why the investigation of this  $k$ -space region with ARPES has been so controversial: in addition to the weakly dispersive SS feature (Fig. 1 and 2), there are several sheets of FS (primary and 'folded'). At this point, the obvious question is: what is the nature of the SS feature (which is not a result of the mere band folding as the SB peaks)? It has been proposed that it could be a surface state [9]. In order to verify this hypothesis, we investigated its sensitivity to surface degradation by cycling the temperature between 10 and 200 K. We observed that the SS peak is suppressed much faster than all other features, including the SB. Furthermore, by cleaving the crystals at 180 K and immediately cooling to 10 K we completely suppressed the SS, affecting the intensity of the other electronic states only weakly. A more sizable effect is observed on the SB, confirming a certain degree of surface degradation. However, this degradation was not too severe, as demonstrated by the LEED pattern taken after the measurements which still clearly shows the surface reconstruction (Fig. 4d). M-region EDC's measured at 10 K (on a sample cleaved at 180 K), and corresponding intensity plots  $I(\mathbf{k}, \omega)$  are shown in Fig. 4a and 4b. No signature of the SS is detected, and the identification of the Fermi vectors of  $\alpha$ ,  $\beta$ , and  $\gamma$  pockets is now straightforward. Performing a complete mapping on a sample cleaved at 180 K, we obtained an extremely well defined FS (Fig. 4c). With the surface slightly degraded, we expect to see less of the relative intensity coming from

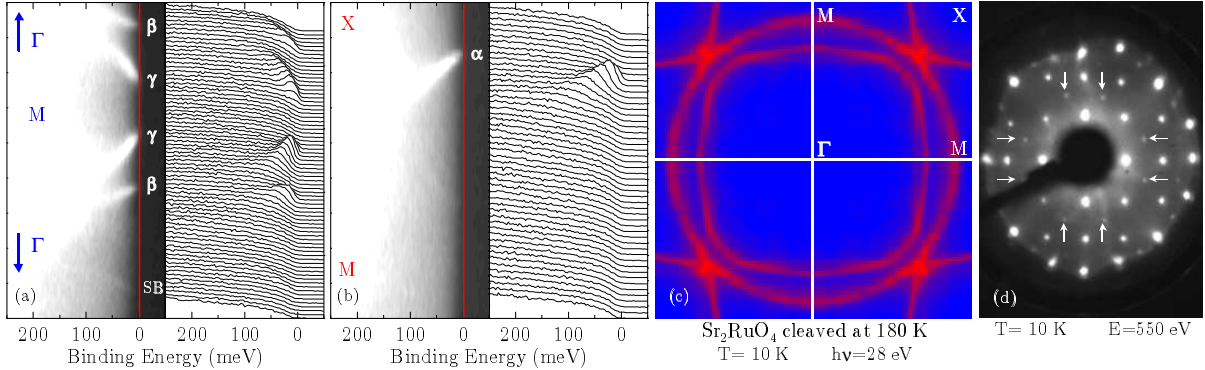


FIG. 4. EDC's and intensity plot  $I(\mathbf{k}, \omega)$  along  $\Gamma$ -M- $\Gamma$ , and M-X (panel a and b, respectively). Panel c:  $E_F$  intensity map. Panel d: LEED pattern recorded at the end of the FS mapping. All data was taken at 10 K on  $\text{Sr}_2\text{RuO}_4$  cleaved at 180 K.

SB and SS (note that the intensity scales in Figs. 3b and 4c, although not displayed, are identical). At the same time, we would expect also the primary FS to be less well defined, which is precisely *opposite* to what is observed. The FS shown in Fig. 4c is in very good agreement with LDA calculations [2,3] and dHvA experiments [4–6]. The number of electrons contained in the FS adds up to a total of 4 (within an accuracy of 1%), in accordance with the Luttinger theorem [13]. In addition, we can confirm that  $\alpha$  and  $\beta$  FS present the nested topology which has been suggested [14] as the origin of the incommensurate magnetic spin fluctuations later observed [15] in inelastic neutron scattering experiments at  $\mathbf{Q} \approx (2\pi/3a, 2\pi/3a, 0)$ .

Our results confirm the surface state nature of the SS peak detected at the M point. The comparison of Figs. 3b and 4c suggests that a surface contribution to the total intensity is responsible also for the less well defined FS observed on samples cleaved at 10 K. At this point, one might speculate that these findings are a signature of the surface ferromagnetism (FM) proposed for  $\text{Sr}_2\text{RuO}_4$  [11]. In this case, two different FS's should be expected for the two spin directions [11], resulting in: (i) additional  $E_F$ -weight near M due to the presence of a *hole-like*  $\gamma$  pocket for the majority spin; (ii) overall momentum broadening of the FS contours because the  $\alpha$ ,  $\beta$  and  $\gamma$  sheets for the two spin populations are slightly displaced from each other in the rest of the BZ. Moreover, due to the surface-related nature of this effect, it would have escaped detection in dHvA experiments. In this scenario, a slight degradation of the surface would significantly suppress the signal related to FM correlations, due to the introduced disorder. The resulting FS would be representative of the non-magnetic electronic structure of the bulk (Fig. 4c). The hypothesis of a FM surface seems plausible because the instability of a non magnetic surface against FM order is not only indicated by *ab initio* calculations [11], but it may also be related to the lattice instability evidenced by the surface reconstruction. To further test this hypothesis, we suggest spin-polarized photoemission experiments.

In summary, our investigation confirms the surface state nature of the weakly dispersive feature detected at the M point (a possible fingerprint of a ferromagnetic surface). On the basis of both ARPES and LEED, we found that a  $\sqrt{2} \times \sqrt{2}$  surface reconstruction occurs in cleaved  $\text{Sr}_2\text{RuO}_4$ , resulting in the folding of the primary electronic structure. Taking these findings into account, the FS determined by ARPES is consistent with dHvA results, providing additional information on the detailed shape of  $\alpha$ ,  $\beta$  and  $\gamma$  pockets.

We gratefully acknowledge C. Bergemann, M. Braden, Ismail, and T. Mizokawa for useful discussions. SSRL is operated by the DOE office of Basic Energy Research, Division of Chemical Sciences. The office's division of Material Science provided support for this research. The Stanford work is also supported by NSF grant DMR9705210 and ONR grant N00014-98-1-0195.

---

- [1] Z.-X. Shen, and D.S. Dessau, Phys. Rep. **253**, 1 (1995).
- [2] T. Oguchi, Phys. Rev. B **51**, 1385 (1995).
- [3] D.J. Singh, Phys. Rev. B **52**, 1358 (1995).
- [4] A.P. Mackenzie *et al.*, Phys. Rev. Lett. **76**, 3786 (1996).
- [5] A.P. Mackenzie *et al.*, J. Phys. Soc. Jpn. **67**, 385 (1998).
- [6] C. Bergemann *et al.*, Phys. Rev. Lett. **84**, 2662 (2000).
- [7] D.H. Lu *et al.*, Phys. Rev. Lett. **76**, 4845 (1996).
- [8] T. Yokoya *et al.*, Phys. Rev. B **54**, 13311 (1996).
- [9] A.V. Puchkov *et al.*, Phys. Rev. B **58**, R13322 (1998).
- [10] A. Liebsch, and A. Lichtenstein, Phys. Rev. Lett. **84**, 1591 (2000).
- [11] P.K. de Boer, and R.A. de Groot, Phys. Rev. B **59**, 9894 (1999).
- [12] R. Matzdorf *et al.*, Science **289**, 746 (2000).
- [13] For the FS determined on samples cleaved at 10 K the accuracy in the electron counting reduces to 3% due to the additional intensity of folded bands and surface state.
- [14] I.I. Mazin, and D.J. Singh, Phys. Rev. Lett. **82**, 4324 (1999).
- [15] Y. Sidis *et al.*, Phys. Rev. Lett. **83**, 3320 (1999).